Acta Histochemica 115 (2013) 728–739

Contents lists available at ScienceDirect

Acta Histochemica

journal homepage: www.elsevier.de/acthis

Hepatitis B virus X antigen and aflatoxin B1 synergistically cause hepatitis, steatosis and liver hyperplasia in transgenic zebrafish

Jeng-Wei Lu[a,b], Wan-Yu Yang[a], Yueh-Min Lin[c], Shiow-Lian Catherine Jin[b], Chiou-Hwa Yuh[a,d,e,*]

[a] Institute of Molecular and Genomic Medicine, National Health Research Institutes, Zhunan, Miaoli, Taiwan
[b] Department of Life Sciences, National Central University, Jhongli City, Taoyuan, Taiwan
[c] Department of Pathology, Changhua Christian Hospital, Changhua City, Changhua County, Taiwan
[d] Institute of Bioinformatics and Structural Biology, National Tsing Hua University, Hsinchu, Taiwan
[e] Department of Biological Science and Technology, National Chiao Tung University, Hsinchu, Taiwan

ARTICLE INFO

Article history:
Received 27 December 2012
Received in revised form 14 February 2013
Accepted 18 February 2013

Keywords:
Hepatitis B virus X antigen
Aflatoxin B1
Liver diseases
Hyperplasia
Transgenic zebrafish

ABSTRACT

Aflatoxin B1 (AFB1) and the hepatitis B virus X antigen (HBx) are linked to the formation of liver diseases and hepatocellular carcinoma (HCC). The aim of this study was to investigate the synergistic effects between HBx and AFB1 in causing liver disorders using a transgenic zebrafish animal model. Histopathology, Periodic acid-Schiff (PAS) staining, Sirius red staining, TdT-mediated dUTP Nick End Labeling (TUNEL) assay, immunohistochemistry, and quantitative reverse transcriptase-polymerase chain reaction (Q-RT-PCR) were used to examine the livers of the HBx transgenic fish injected with AFB1. We found that HBx and AFB1 synergistically promoted steatosis as indicated by histopathological examinations and the increased expression of lipogenic factors, enzymes, and genes related to lipid metabolism. Moreover, treatment of AFB1 in HBx transgenic fish accelerated the development of liver hyperplasia and enhanced the expression of cell cycle related genes. PCNA was co-localized with active caspase 3 protein expression in HBx zebrafish liver samples and human HBV positive HCC samples by double fluorescence immunostaining. Finally, we found that in human patients with liver disease, significant glycogen accumulated in the inflammation, cirrhosis stage, and all cases of hepatocellular and cholangiocellular carcinoma showed a moderate cytoplasmic accumulation of glycogen. Our data demonstrated a synergistic effect of AFB1 and HBx on the regulation of lipid metabolism related genes and cell cycle/division-related genes which might contribute to enhanced steatosis and hyperplasia at 5.75 months.

© 2013 Elsevier GmbH. All rights reserved.

Introduction

Hepatocellular carcinoma (HCC) is the most common malignancy in East Asia and Africa. Hepatocarcinogenesis is a multistep process involving steatosis, fibrosis, cirrhosis, adenoma, and carcinoma (Tarantino et al., 2007). HCC is commonly associated with chronic hepatitis B virus (HBV) or hepatitis C virus (HCV) infections or chronic exposure to AFB1 and is a complication of alcoholic cirrhosis (Morgan et al., 2004; McGlynn and London, 2005; Seeff and Hoofnagle, 2006; El-Serag and Rudolph, 2007; Marrero and Marrero, 2007). Treatment options for liver cancer are currently limited, and the prognosis is generally poor and five year survival rate after surgery is limited (Lu et al., 2011). Therefore, HCC remains one of the deadliest cancers, with a 5-year survival rate of only 5% (El-Serag et al., 2001). Many risk factors, such as the HBx and AFB1-induced genetic and epigenetic alterations in hepatocytes, result in the transformation into neoplasia (Roberts, 2008; Siegel et al., 2010). However, the synergies between the various risk factors that result in HCC are unclear. The aim of present study was to identify the potential synergistic effects between HBx and AFB1 in promoting liver disease and HCC development and to understand the underlying mechanism using a zebrafish model.

Chronic HBV infection has been shown to be strongly associated with HCC (Beasley et al., 1981; Robinson, 1992; Brechot, 2004). One of the viral antigens of HBV that has shown an oncogenic role is HBx, which is present in the cytoplasm and, to a lesser extent, the nucleus of hepatocytes (Kew, 2011). HBx communicates with a variety of host targets and mediates many opposing cellular functions, including cell cycle regulation, apoptosis, signaling and transcriptional regulation and affects many molecules including cytoskeletal and cell adhesion molecules, oncogenes and tumor suppressor genes (Peng et al., 2005; Pang et al., 2006). AFB1 is a mycotoxin produced by *Aspergillus flavus* and related fungi that grow on crops including corn, rice and peanut (Bennett and Klich, 2003). It is metabolized predominantly in the liver to AFB1-8,9-exo-epoxide, which forms a promutagenic AFB1-N7-guanine DNA adduct that results in G–T transversion mutations (Wild and Turner,

* Corresponding author at: Institute of Molecular and Genomic Medicine, National Health Research Institutes, Zhunan, Miaoli, Taiwan.
E-mail address: chyuh@nhri.org.tw (C.-H. Yuh).

0065-1281/$ – see front matter © 2013 Elsevier GmbH. All rights reserved.
http://dx.doi.org/10.1016/j.acthis.2013.02.012

2002). AFB1 has gained much attention as one of the most prevalent carcinogens (Akriviadis et al., 1998). Mutational inactivation of the p53 gene has been well described to be one of the molecular mechanisms involved in HCC pathogenesis, especially in geographical areas where dietary AFB1 exposure is more serve (Hsu et al., 1991; Aguilar et al., 1994; Pang et al., 2006). Different animal models have been used to examine the interaction between the hepatitis virus and AFB1 exposure, but, in general, these have suffered from a number of limitations (Wild et al., 1993). In the HBx and HCV transgenic mice, AFB1 treatment induced significantly more liver tumors than in wild-type mice (Lian et al., 2006; Jeannot et al., 2011). More importantly, hepatic oval cells (HOC) which are considered as liver stem cells, after transfection with HBx gene and implantation into mice, produce tumors in the animal treated with aflatoxin B1 (16.7%) in the liver (Li et al., 2011). This result provided evidence for the combined effect between HBx and AFB1.

In the present study, we used the liver fatty acid-binding protein (*l-fabp*) promoter to drive HBx expression specifically in the liver (Andre et al., 2000; Denovan-Wright et al., 2000). The protein product of *l-fabp* binds to long chain fatty acids in hepatocytes and is responsible for their trafficking. The zebrafish *l-fabp* promoter faithfully drives GFP expression in the liver (Her et al., 2003). The hepatotoxin AFB1 was administered *via* intraperitoneal injection, as shown previously. To the best of our knowledge, the collaborative effect of HBx and AFB1 in causing liver disease using a transgenic zebrafish model has not been reported. Therefore, we used histopathology, PAS staining, Sirius red staining, TUNEL assay, immunohistochemistry, and Q-RT-PCR in the present study to examine the synergistic effect of HBx and AFB1 in promoting liver disease and explore the possible mechanisms that underlie those disorders.

Materials and methods

Zebrafish maintenance

Zebrafish were maintained in the Zebrafish core facility at NTHU-NHRI (ZeTH) according to established protocols (Tseng et al., 2011). The Tg(*l-fabp*:GFP-mCherry) and Tg(*l-fabp*:HBx-mCherry) transgenic embryos, larvae, and adult fish were maintained at 28 °C under continuous flow in the Zebrafish Core Facility with automatic control for a 14-h light and 10-h dark cycle. All experiments involving zebrafish were approved by the Institutional Animal Care and Use Committee (IACUC) of the NHRI (NHRI-IACUC-101005-A). The liver-specific transgenic fish were generated as described previously (Kwan et al., 2007).

AFB1 treatment, liver tissue collection, and paraffin sectioning

According to a previous study, AFB1 can be dissolved in 8% DMSO, and the vehicle itself does not have any toxicity to liver or animal survival (Luyendyk et al., 2003). AFB1 (Acros Organics, Thermo Fisher Scientific, Geel, Belgium) was dissolved in 8% DMSO to a final concentration of 0.15 μg/μl and injected with 10 μl. AFB1 induces HCC in a mouse model with a single dose of 3 mg/kg injected intraperitoneally (Hiruma et al., 2001). Because each zebrafish weighs approximately 0.5 g, we injected 1.5 μg of AFB1 per fish. Transgenic zebrafish of 2.75 months of age were injected intraperitoneally with the AFB1 solution (1.5 μg/10 μl). Transgenic fish were sacrificed at 1, 3, 6, 9 and 12 weeks post-AFB1 injection. The tissues were frozen in liquid nitrogen immediately after dissection and stored at −70 °C for later RNA extraction. For histochemical analysis, liver tissues were fixed in a 10% formalin solution (Sigma–Aldrich, St. Louis, MO, USA). The fixed tissue was embedded in paraffin, sectioned at 5-μm thickness, and mounted on poly-L-lysine coated slides. Following deparaffinization, the sections were stained with hematoxylin and eosin. Diagnosis was performed by using a single-blind evaluation of all samples by trained pathologists (Dr. Yueh-Min Lin, Changhua Christian Hospital, Changhua, Taiwan). There are 57 samples representing five different stages for four groups (no AFB1 + no HBx, HBx alone, AFB1 alone and AFB1 + HBx). The numbers of biological replicates were variable for each stage and group, and the details are listed in Supplementary Table 1.

Histochemical analysis

Paraffin-embedded tissue sections slides were deparaffinized. The slides were treated with 3% H_2O_2 to block endogenous peroxidase activity, and heated in 10 mM citrate buffer at 100 °C for 30 min to retrieve antigen. The sections were incubated at 4 °C overnight with different primary antibodies including rabbit anti-active caspase 3 (1:100 dilution; BD Biosciences, Le Pont-de-Claix, France), mouse anti-PCNA (1:100 dilution; Santa Cruz Biotechnology, Santa Cruz, CA, USA), mouse anti-HBx (1:100 dilution; Abcam, Cambridge, MA, USA), and mouse anti-AFB1-DNA adduct (1:100 dilution; Novus Biologicals, LLC, Littleton, CO, USA). After washing with 1× PBS, the sections were incubated with a secondary antibody for 30 min at room temperature, which was followed by development using the Liquid DAB Substrate Kit (Invitrogen, Carlsbad, CA, USA). Tissue sections were counterstained with hematoxylin, dehydrated, clear, mounted and examined by light microscopy. For double fluorescent immunohistochemistry, sections were incubated at 4 °C overnight with primary antibodies, including rabbit anti-active caspase 3 (1:100 dilution; BD Biosciences, Le Pont-de-Claix, France), mouse anti-PCNA (1:100 dilution; Santa Cruz Biotechnology, Santa Cruz, CA, USA). After washing with 1x PBS, the sections were incubated with goat anti-rabbit IgG or goat anti-mouse IgG rhodamine (FRITC) secondary antibodies (1:100 dilution; both from Jackson ImmunoResearch (West Grove, PA, USA) for 60 min at room temperature. Tissue sections were mounted and examined by fluorescent microscopy. Sirius red staining was performed using the Picrosirius Red Stain Kit (Polysciences, Warrington, PA, USA) to detect collagen fibers. The glycogen accumulation was detected using the Periodic acid-Schiff (PAS) Stain Kit (Polysciences). TUNEL assay was performed using the *In Situ* Cell Death Detection Kit, Fluorescein (Roche, Indianapolis, IN, USA) according to the manufacturer's instructions. The tissue sections then were dehydrated, cleared, mounted and examined by light or fluorescent microscopy. We scored the Sirius red staining and TUNEL assay results by intensity, which ranged from negative (0) to minimal (1), moderate (2), and maximal (3). The staining intensity for PAS, caspase 3 and PCNA were scored as 0 (0–15%), 1 (16–25%), 2 (26–50%), or 3 (76–100%) according to the percentage of positively stained cells (Fig. S1).

Human liver disease spectrum tissue microarray

To investigate the relationship of glycogen accumulation with human liver disease, we purchased the human liver disease tissue array for PAS staining. The liver disease spectrum tissue microarray (catalog #: BC03002) was purchased from US Biomax (Rockville, MD, USA). Each array contains 15 primary HCCs, 8 cholangiocellular carcinomas, 8 samples of liver cirrhosis, 5 liver samples with the hepatitis virus and 2 normal adjacent liver samples, duplicate cores per case. Periodic acid-Schiff (PAS) staining for glycogen accumulation was performed as described in the previous section.

RNA isolation and quantitative RT-PCR

Total RNA was isolated by the RNAspin Mini RNA Isolation Kit (GE Healthcare, Pittsburgh, PA, USA). RNA (1 μg) was reverse transcribed into cDNA using the High Capacity RNA-to-cDNA Kit (Applied Biosystems, Carlsbad, CA, USA). The resulting first-strand cDNA was used as a template for qualitative PCR in triplicate using the SYBR Green Q-PCR Master Mix Kit (Applied Biosystems). Oligonucleotides PCR primer pairs were designed to cross intron-exon boundaries from published sequences in the GeneBank database using Primer3. Primers were purchased from a Taiwanese company (Mission Biotech, Taipei, Taiwan, ROC) and the oligonucleotides were column purified and salt free.

We chose some markers for genes involved in the hepatic lipid accumulation, fibrosis, cell cycle and tumor from literature based on a previous study on HBx transgenic fish (Rekha et al., 2008; Shieh et al., 2010). The sequence of primers for Q-PCR is provided in Supplementary Table 2. The specificity of the amplification products was confirmed by size estimations on a 1.2% agarose gel and by analyzing their melting curves. A primer dimer was ruled out by performing a "no template" control and analyzing the dissociation curve, and the without template, no cycle (Cq) values could be determined. After normalization to internal control actin or 18S, the expression ratio between the experimental and control groups was calculated using the comparative Ct method. All experiments were performed in triplicate, and the means of three values are presented. At least three independent samples were used for Q-PCR, and the standard error was calculated and incorporated into the presented data as medians ± standard error. For absolute molecules analysis shown in Fig. 1, the RNA molecules per embryo was calculated using the standard curve as described earlier (Chan et al., 2009; Tseng et al., 2011). Briefly, a series of known amount of GFP fragment was used for Q-PCR and standard curve of RNA molecules verse Ct was generated, the Ct of HBx from Q-PCR analysis was converted into RNA molecules using the standard curve.

Statistics

Statistical analysis of human glycogen accumulation and Q-PCR results was performed using the unpaired Student's *t*-test. Cumulative frequency of the pathology changes in transgenic zebrafish was calculated by Kaplan–Meier analysis (Zhu et al., 2012). In all statistical analyses, a *p*-value of less than 0.05 was considered to be statistically significant.

Results

Expression of the HBx-mCherry fusion protein and formation of AFB1-DNA adducts in transgenic fish

To investigate the interplay between HBx and AFB1 in liver disease, we used the liver-specific *l-fabp* promoter to drive expression of the GFP-mCherry or HBx-mCherry fusion protein in zebrafish. Two different sizes of *l-fabp* were used: 2264 bp (attB4-*l-fabp*-F1 + attB1r-*l-fabp*-R for GFP-mCherry) and 2870 bp (attB4-*l-fabp*-F + attB1r-*l-fabp*-R for HBx-mCherry), and both of them can drive the fusion protein in the liver as described below. We first examined the expression of the fusion protein using fluorescence microscopy. The livers of three-month-old adults exhibited green and red fluorescence for the F1 founder carrying *l-fabp*:GFP-mCherry or red fluorescence for the F1 founder carrying *l-fabp*:HBx-mCherry (Fig. 1A). Using Q-PCR for absolute quantification, we found that the HBx RNA expression level in the livers of HBx transgenic fish decreased steadily over time (Fig. 1B), which is similar to the results shown in the HBx transgenic mouse (Lu et al., 2012). The expression of the HBx protein was further verified by immunohistochemistry using an anti-HBx antibody. In contrast to the EGFP-mCherry transgenic fish that showed no HBx expression, hepatocytes from HBx transgenic fish showed a strong expression of the HBx protein from 3 to 5.75 months of age (Fig. 1C). In a total of 57 liver samples, a successful AFB1 treatment was verified using an antibody specific for the AFB1-DNA adduct, which was continuously present in the hepatocytes at even 12 weeks post-treatment, but not in the HBx transgenic fish that were not treated with AFB1 (Fig. 1D).

Histopathological examination of synergistic effect of HBx and AFB1 in the transgenic zebrafish model

Previous studies showed that HBx overexpression in the zebrafish liver caused hepatic steatosis and liver degeneration, but no signs of HCC (Shieh et al., 2010). A synergistic interaction between chronic HBV infection and AFB1 in hepatocarcinogenesis was previously reported (Kew, 2003). To increase the chance of HCC formation in zebrafish, we intraperitoneally injected 2.75-month-old transgenic fish (expressing GFP-mCherry or HBx-mCherry) with AFB1 and collected the livers at 1, 3, 6, 9 and 12 weeks post-injection (wpi) for analysis. A total of 57 samples were collected from different treatment groups, and detailed information regarding the histopathological examination of these specimens is listed in Supplementary Table 2.

Compared to the control Tg(*l-fabp*:GFP-mCherry) fish (Fig. 2A1–A5), hepatocytes from the Tg(*l-fabp*:HBx-mCherry) fish displayed steatosis, inflammation, and balloon degeneration from 3 to 5.75 months of age (Fig. 2B1–B5). These observations are consistent with previous reports (Shieh et al., 2010). AFB1 alone promoted hepatitis or steatosis development starting from 6 wpi (or 4.25 months of age) (Fig. 2C1–C5). Moreover, AFB1 and HBx synergistically promoted hepatocyte steatosis as early as 1 wpi (Fig. 2D1), and the fish developed hepatitis and steatosis from 3 to 9 wpi (Fig. 2D2–D4), while finally hyperplasia was observed at 5.75 months of age, which corresponds to 12 weeks after the AFB1 treatment (Fig. 2D5). The cumulative frequency analysis of the H&E staining results from multiple HBx transgenic fish lines is summarized in Fig. 2E. Although HBx and AFB1 alone can induce hepatitis (Fig. 2E1) and steatosis, an increasing number of fish developed steatosis with the presence of both factors (Fig. 2E2). Approximately 20% of the HBx transgenic fish treated with AFB1 developed hyperplasia (Fig. 2E3) at 5.75 months of age.

For additional pathological changes, the liver sections of the AFB1-treated HBx transgenic fish were stained with Sirius red and periodic acid-Schiff (PAS) stain to detect the deposition of extracellular matrix and glycogen accumulation, respectively. The terminal deoxynucleotidyl transferase dUTP nick end labeling (TUNEL) assay was performed to examine apoptosis, staining with an antibody to active caspase 3 was used to detect activated apoptosis, and staining with an antibody to the proliferating cell nuclear antigen (PCNA) was used to analyze cell proliferation. Multiple samples from each stage of the different zebrafish lines were used for these analyses, and the scoring was standardized by comparing the percentage of cells with the staining as shown in Fig. S1.

According to the result of PAS staining, HBx overexpression combined with the AFB1 treatment caused an increase in glycogen accumulation, although HBx and AFB1 alone could also enhance glycogen accumulation (Fig. 3A). As indicated by Sirius red staining, HBx and AFB1 alone can promote fibrosis, and there does not appear to be any synergistic effect between them (Fig. 3B). Cell proliferation, as indicated by nuclear PCNA staining, gradually increased in the HBx and AFB1 alone fish, however, AFB1 treated HBx transgenic fish had the strongest PCNA staining at score 3 (Fig. 3C). From TUNEL assay, zebrafish overexpressing HBx or that was treated with AFB1 had significantly more apoptotic cells than the control fish, and

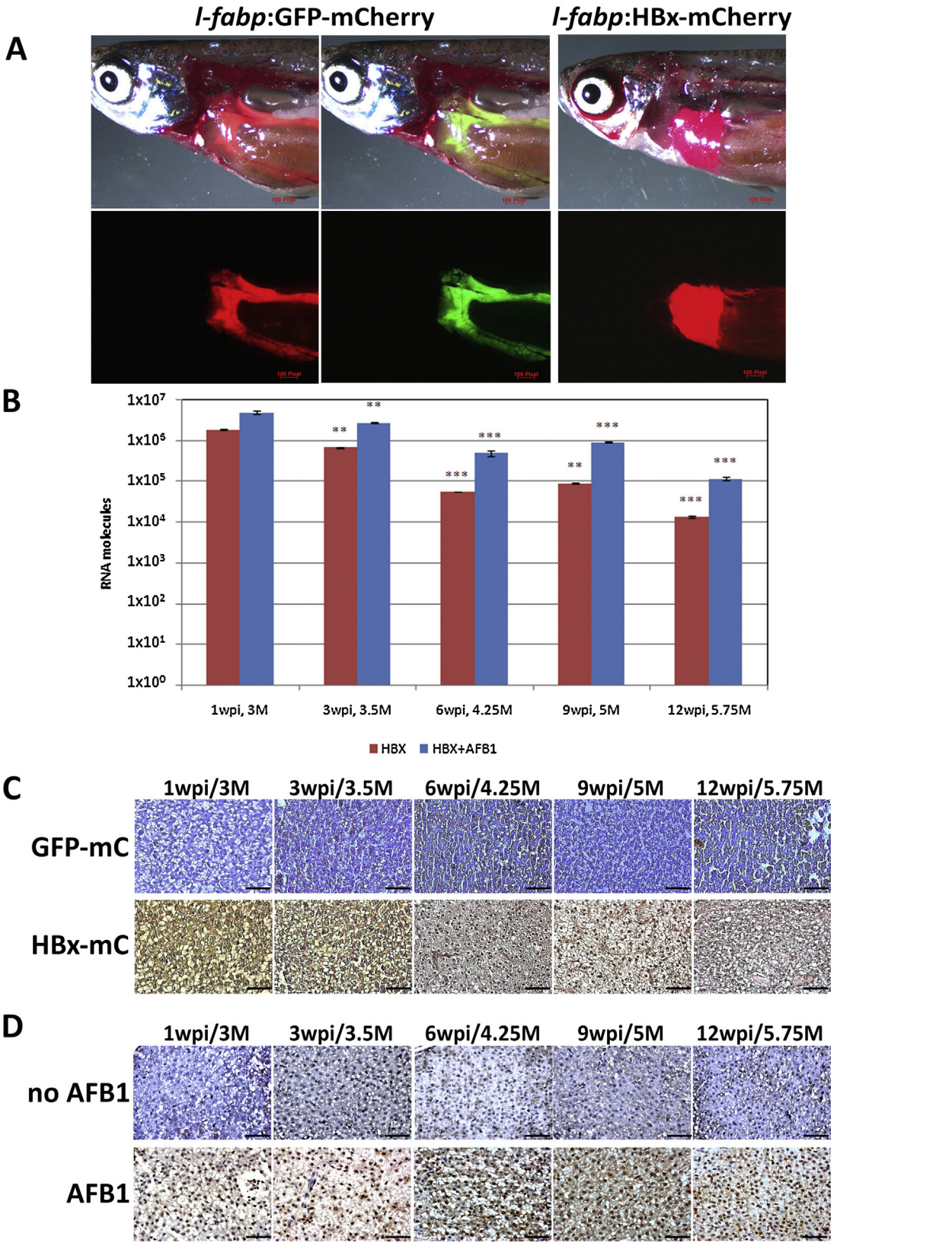

Fig. 1. Expression of the HBx-mCherry fusion protein and HBx and the formation of AFB1-DNA adduct in the transgenic fish. (A) The EGFP-mCherry fusion protein was expressed in the liver, as indicated by both the green and red fluorescence detected in the liver of a wild-type fish containing the *l-fabp*:GFP-mCherry transgene. The HBx-mCherry fusion protein was expressed in the liver of the *l-fabp*:HBx-mCherry transgenic fish, as indicated by the red fluorescence. (B) Q-RT-PCR analysis of the expression of HBx RNA in the liver tissue of HBx-mCherry transgenic fish without (red column) or with AFB1 treatment (blue column) at 3, 3.5, 4.25, 5 and 5.75 months of age. (C) Immunohistochemical analysis of the expression of the HBx protein in hepatocytes from the 3-, 3.5-, 4.25-, 5- and 5.75-month-old HBx-mCherry transgenic fish and control EGFP-mCherry transgenic fish (400×). (D) Immunohistochemistry for the presence of the AFB1-DNA adduct in the hepatocytes of HBx-mCherry transgenic fish at 1, 3, 6, 9 and 12 weeks post-AFB1 injection (wpi), which were compared to the fish without the AFB1 treatment (400×). Scale bars = 50 μm. (For interpretation of the references to color in this figure legend, the reader is referred to the web version of the article.)

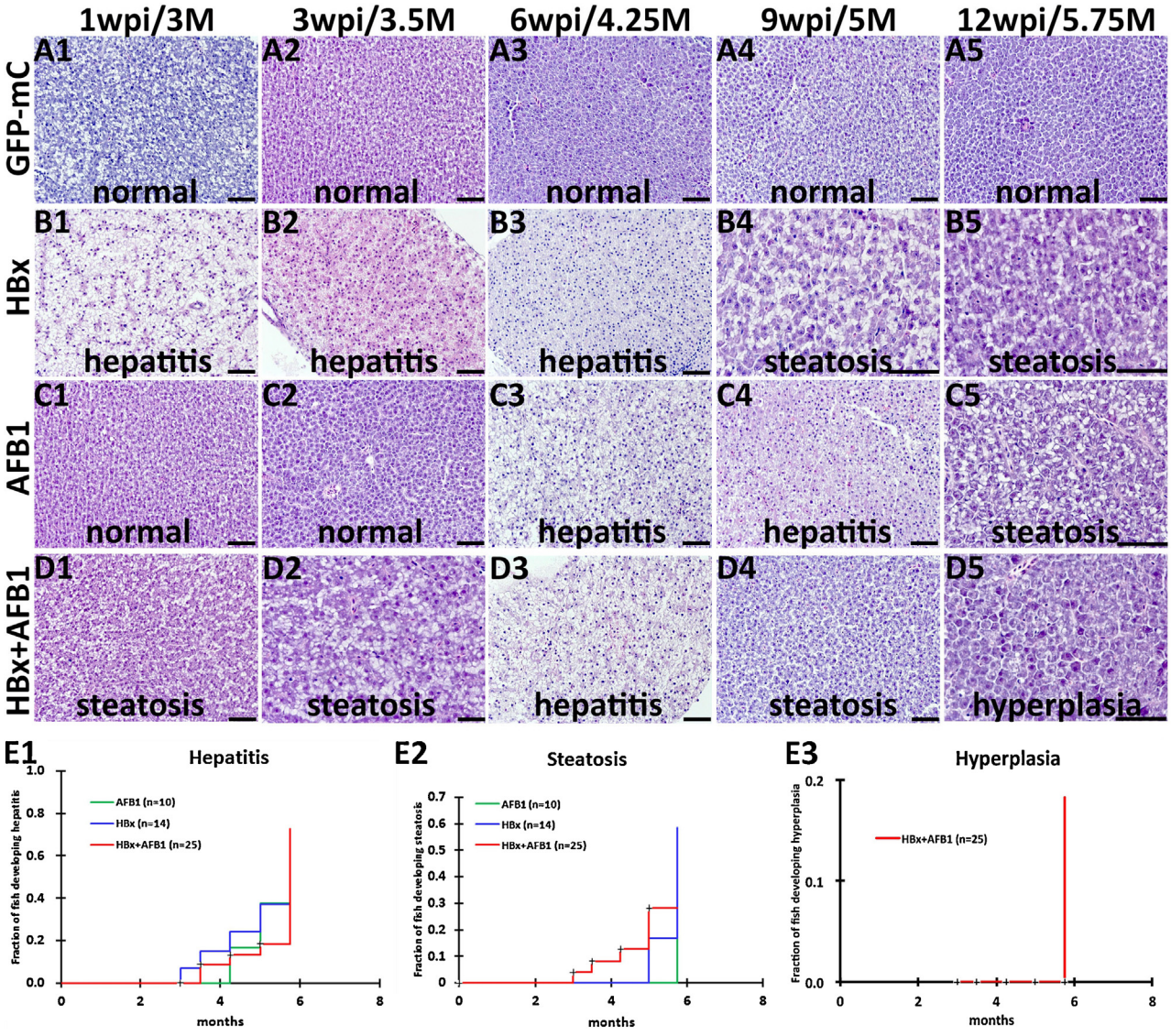

Fig. 2. Histopathology of hepatocytes affected by HBx and AFB1 at five different stages. Liver sections were prepared from (A) GFP-mCherry transgenic fish, (B) HBx transgenic fish, (C) AFB1-treated GFP-mCherry fish, and (D) AFB1-treated HBx transgenic fish (400× or 200×). The fish were 3, 3.5, 4.25, 5 or 5.75 months old or 1, 3, 6, 9, or 12 weeks post-AFB1 injection (wpi). Scale bars: 50 μm. (E) Cumulative frequency of hepatitis (E1), steatosis (E2) or hyperplasia (E3) from multiple lines of transgenic fish by Kaplan–Meier analysis. Green line indicated AFB1 treated GFP-mCherry transgenic fish, blue line denoted HBx transgenic fish and red lines represented AFB1 treated HBx transgenic fish. (For interpretation of the references to color in this figure legend, the reader is referred to the web version of the article.)

there appeared to be no synergistic effect between these two conditions (Fig. 3D). The caspase 3 staining results similar to the TUNEL assay (data not show). Taken together, these data suggest that HBx and AFB1 have a synergistic effect on glycogen accumulation and cell proliferation. However, while each condition can induce fibrosis and apoptosis, there was no additive effect when the two factors were combined.

Glycogen accumulation occurred in the inflammation stage and reappeared in the hyperplasia stage

We found significant glycogen accumulation in the hepatocytes from both the early stage (1, 3, 6 weeks post-injection) of HBx transgenic fish and the late stage (9 and 12 weeks post-injection) of HBx transgenic fish treated with AFB1. To identify the correlation of glycogen accumulation with human liver disease, we used the tissue array for PAS staining. PAS stain results showed that glycogen accumulation at different levels in different samples that can be scored into four classes according to the percentage of positively stained cells (Fig. 4A). In human patients with liver disease, the correlation between glycogen accumulation and liver disease was calculated by *t*-test and the following stages showed significant differences ($P < 0.001$): inflammation, cirrhosis, stages II and III of hepatocellular and cholangiocellular carcinoma. However, stage I of hepatocellular and cholangiocellular carcinoma showed a moderate cytoplasmic accumulation of glycogen. By comparing the PAS staining from humans and zebrafish with liver diseases, we observed dramatically similar phenomena for the glycogen accumulation that occurred in the inflammation stage and reappeared in the highly proliferative stage (Fig. 4B).

Synergistic effect of HBx and AFB1 on the expression of lipogenic factors and cell cycle-related genes

We further used Q-PCR to quantify the expression of marker genes that represent different liver diseases (Fig. 5). The choice of lipogenic genes involved in the hepatic lipid accumulation was followed previous study on HBx transgenic fish (Rekha et al., 2008;

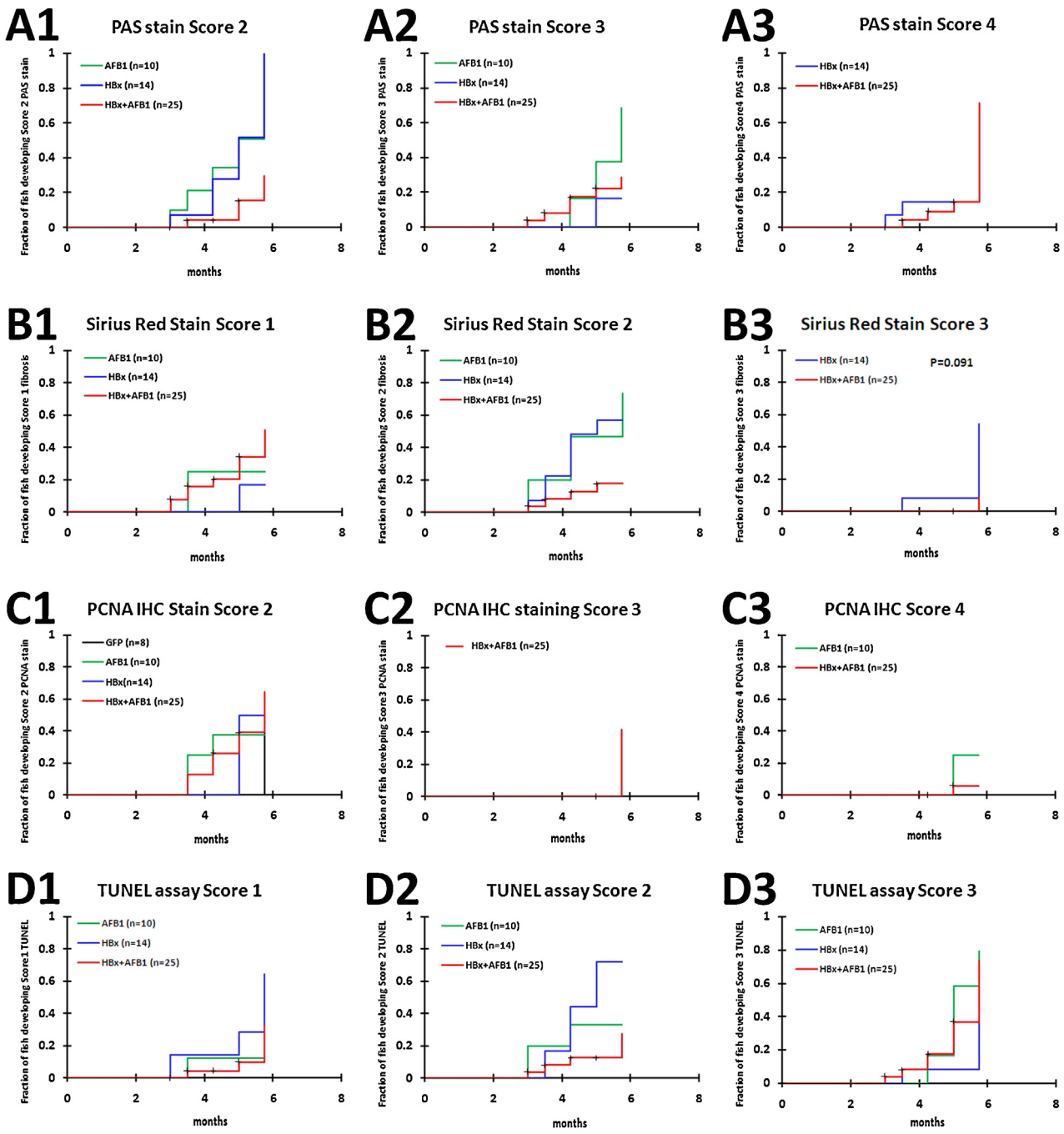

Fig. 3. Cumulative frequency of histochemistry analysis from multiple lines of transgenic fish by Kaplan–Meier analysis. (A) Statistical analysis of periodic acid-Schiff (PAS) staining for glycogen accumulation. (B) Statistical analysis of the fibrosis analysis by Sirius red staining. (C) IHC staining for nuclear PCNA. (D) Statistical analysis of the TUNEL assay for apoptosis. Green line indicated AFB1 treated GFP-mCherry transgenic fish, blue line denoted HBx transgenic fish and red lines represented AFB1 treated HBx transgenic fish. The intensity of each staining was shown on top as score 1–4, respectively. The five stages are 3, 3.5, 4.25, 5 and 5.75-month-old fish or 1, 3, 6, 9, and 12 weeks post-AFB1 injection (wpi). (For interpretation of the references to color in this figure legend, the reader is referred to the web version of the article.)

Shieh et al., 2010). Corresponding to the pathological features in which steatosis developed at between 5 and 5.75 months, the PCR results showed that most of the lipid metabolism related genes are up-regulated more significantly in HBx and AFB1 together than each factor alone (Fig. 5A–D).

Important transcription factors involved in fatty acid synthesis includes cebpα (CCAAT enhancer binding protein-alpha) which is a bZIP transcription factor, which can bind as a homodimer to certain promoters and enhancers, and transcriptionally activated during adipocytes differentiation, pparγ (peroxisome proliferator-activated receptor gamma) which is nuclear receptor protein that function as transcription factor regulating genes for fatty acid storage and glucose metabolism, srebp1 (sterol regulatory binding protein-1) which encodes a transcription factor that binds to the sterol regulatory element-1 (SRE1) of genes involved in sterol biosynthesis, and chrebp (carbohydrate-response element-binding protein) which is a transcriptional regulator of glucose and lipid metabolism. The lipogenic factors (*pparγ*, *chrebp* and *srebp1*are up-regulated at 5 M, except the *cebpα* which showed much lower expression in all three group (Fig. 5A), and the HBx together with AFB1 exhibit the significant overexpression than each factor alone.

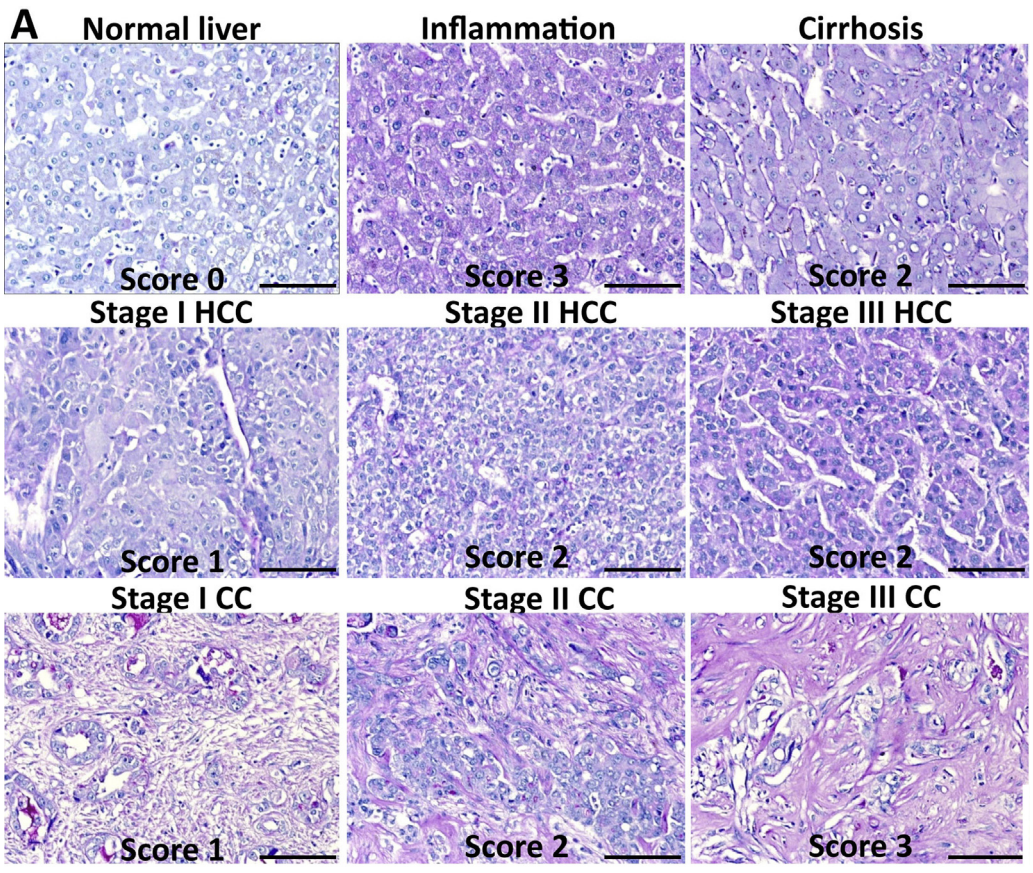

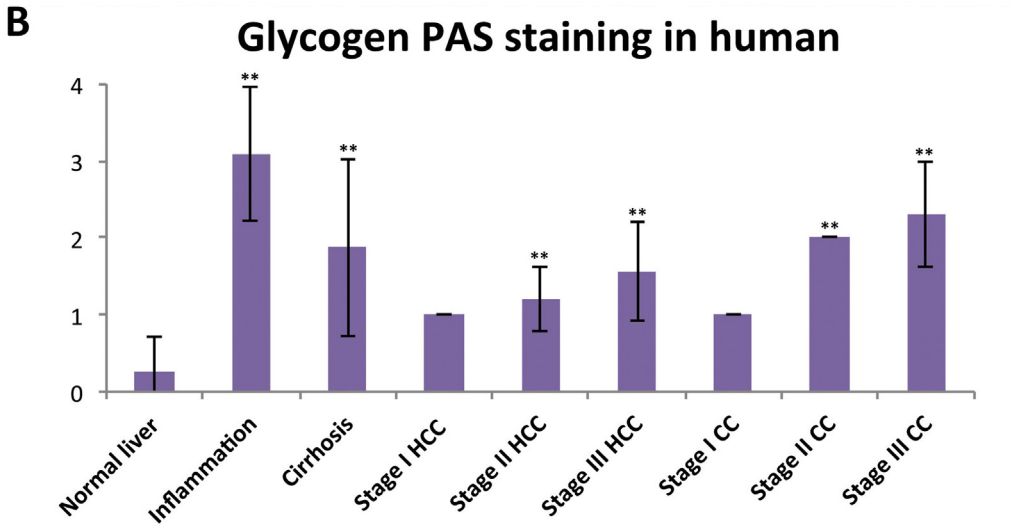

Fig. 4. Periodic acid-Schiff (PAS) staining analysis of human liver disease array at various stages. (A) The glycogen accumulation from different human liver diseases ranged from normal, inflammation, cirrhosis, and stages I–III of hepatocellular carcinoma (HCC) and cholangiocarcinoma (CC) (200×). Scale bars = 50 μm. (B) Each stain result was evaluated and given a score of 0–4, and the average of the scores was obtained from multiple samples of the same stage for the PAS staining. Eighty human liver tissues were purchased as a human tissue array format. The significance was calculated using a *t*-test and shown as "** for $P < 0.001$".

Lipogenic enzyme include key enzyme for fatty acid *de novo* synthesis-fasn (fatty acid synthase), which is a multi-enzyme that plays a key role in fatty acid synthesis; and acacb (ACACB acetyl-CoA carboxylase beta) which converts acetyl-CoA to malonyl-CoA, is the committed step of the fatty acid synthesis pathway. Lipogenic enzyme include agapt (acyl-CoA: 1-acylglycerol-sn-3-phosphate acyl-transferase), pap (phosphatidic acid phosphatase) which is a key enzyme in triglyceride biosynthesis, and dgat2 (diacylglycerol O-acyltransferase 2) which catalyzes the formation of triglycerides from diacylglycerol and Acyl-CoA. Among them, *acacb*, *agapt*, and *pap* are all up-regulated in HBx + AFB1 more than each factor alone, but the *dgat2* does not show synergistic effect, and the *fasn* was not highly expressed in all three groups (Fig. 5B).

The PPAR-γ target genes include CD36, which plays a critical role in fatty acid uptake; ucp2 (mitochondrial uncoupling protein 2) which can protect against oxidative stress-associated neurogenic hypertension; caveolin belongs to a family of integral membrane proteins which are the principal components of caveolae

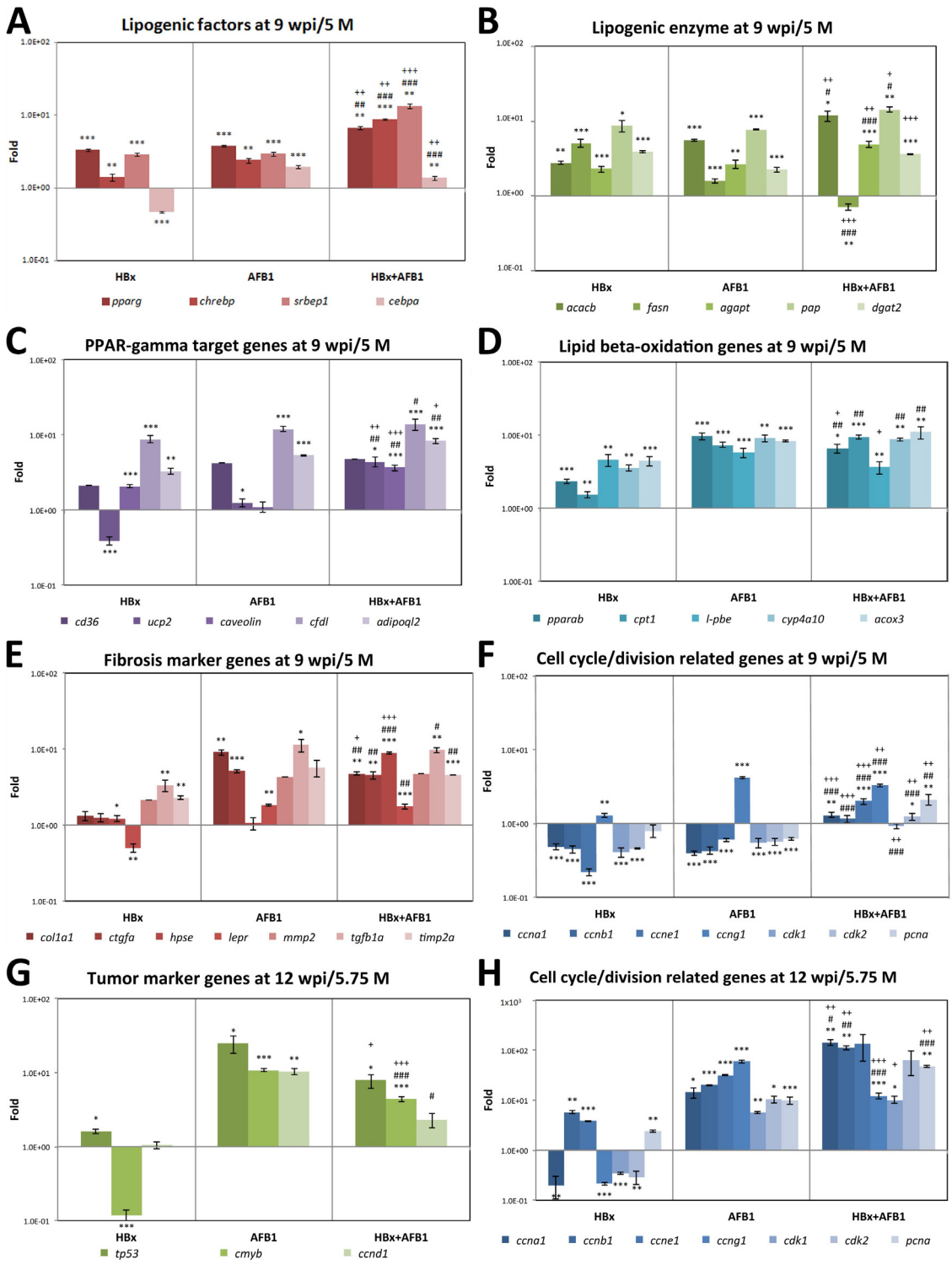

Fig. 5. Quantitative RT-PCR analysis of selected marker genes representing different liver diseases in the HBx, AFB1 and HBx + AFB1 fish. (A) Lipogenic factor, (B) lipogenic enzyme, (C) PPAR-gamma target, (D) lipid beta-oxidation, (E) fibrosis markers, (F) cell cycle/division from fish at 9 wpi/5 M and (G) tumor markers and (H) cell cycle/division from fish at 12 wpi/5.75 M. There are three groups of fish, as follows: HBx transgenic fish (first group), AFB1-treated GFP-mCherry transgenic fish (second group) and AFB1-treated HBx transgenic fish (third group). Each Ct was first normalized against β-actin and then compared to the Ct from the EGFP-mCherry fish. The delta–delta Ct values were then converted to fold differences. Multiple replicates were performed, and the means are shown with standard deviations. The significance was calculated using a *t*-test and shown as "*" when compared to GFP-mCherry transgenic fish, as "+" when HBx + AFB1 was compared to HBx only, or as "#" when HBx + AFB1 was compared to AFB1 only. The significance is indicated as *, +, or # for $0.01 < P \leq 0.05$; **, ++, or ## for $0.001 < P \leq 0.01$; or ***, +++, or ### for $P \leq 0.001$.

membranes and involved in receptor-independent endocytosis; cfdl (complement factor D or adipisin) is the adipocyte serine protease; adipoql2 (adiponectin) is a protein hormone that modulates a number of metabolic processes, including glucose regulation and fatty acid catabolism. Among them, *ucp2*, *carveolin* and *adipoql2* showed significant synergistic effect between HBx and AFB1. The increased of *cd36* is not significant, and the expression of *adipisin* is high in all three groups (Fig. 5C).

The lipid beta-oxidation protein (ppar-β, cpt1 (carnitine palmitoyltransferase 1) which mediates the transport of long-chain fatty

acids across the membrane by binding them to carnitine; l-pbe (L-peroxisomal bifunctional enzyme) which is the second enzyme of the L-hydroxy-specific classical β-oxidation system, cyp4a10 (cytochrome P450, family 4, subfamily a, polypeptide 10) which is the major enzymes involved in drug metabolism and bioactivation, and acox3 (fatty acyl-CoA oxidase (AOX), the first enzyme of the L-hydroxy-specific classical β-oxidation system. All of the lipid beta-oxidation genes were upregulated at 5 months of age in the HBx or AFB1 alone, and seems no synergistic effect between HBx and AFB1 (Fig. 5D).

The choice of fibrosis markers and tumor markers was also based on a previous study using transgenic fish for liver disease study (Rekha et al., 2008). Fibrosis markers which included col1a1 (collagen, type I, alpha 1), atgfa (connective tissue growth factor (CTGF) which mirrors some of the effects of TGF beta on skin fibroblasts, such as stimulation of extracellular matrix production, chemotaxis, proliferation and integrin expression; hpse (heparanase) is an enzyme that acts both at the cell-surface and within the extracellular matrix to degrade polymeric heparan sulfate molecules into shorter chain length oligosaccharides. Other genes related to metastasis included *lepr* (leptin receptor) is a single-transmembrane-domain receptor of the cytokine receptor family functions as a receptor for the fat cell-specific hormone leptin; *mmp2* is the protease responsible for metastasis, *tgfb1a* (transforming growth factor beta 1 alpha) acts synergistically with transforming growth factor alpha in inducing transformation, and *timp2a* (tissue inhibitor of metalloproteinase 2a) maintains connective tissue integrity by modulating MMP activity. Among those genes, most of them were upregulated at 5 months (Fig. 5E), and decreased at 5.75 month. For most of the genes, AFB1 has stronger effect on increasing their expression than HBx alone, and the synergistic effect is most obvious for *col1a1* and *hpse*.

Cell cycle and division related genes include *ccna1*, *ccnb1*, *ccne1*, *ccng1*, *cdk1*, *cdk2* and *pcna*. The eukaryotic cell cycle is governed by cyclin-dependent protein kinases (cdks) whose activities are regulated by cyclins and cdk inhibitors. Cyclin-A1 (ccna1) functions as activating subunits of enzymatic complex together with cyclin-dependent kinases. G2/mitotic-specific cyclin-B1 (ccnb1) is a regulatory protein involved in mitosis. Cyclin E (ccne) binds to G1 phase cdk2, which is required for the transition from G1 to S phase. Cyclin dependent kinase 1 (cdk1) is a highly conserved protein that functions as a serine/threonine kinase, and is a key player in cell cycle regulation. The activity of cyclin-dependent kinase 2 (cdk2) is restricted to the G1-S phase of the cell cycle, and is essential for the G1/S transition. Proliferating cell nuclear antigen (pcna) is an antigen that is expressed in the nuclei of cells during the DNA synthesis phase of the cell cycle. Cell cycle/division-related genes were not upregulated at 5 months of age but were dramatically upregulated at 5.75 months of age (Fig. 5F and H).

Tumor markers include p53 (protein 53 or tumor protein 53) which is important in multicellular organisms, where it regulates the cell cycle and, thus, functions as a tumor suppressor that is involved in preventing cancer and upregulated in many cancer types with mutant forms; c-myb proto-oncogene (cmyb) plays an important role in the control of proliferation and differentiation of hematopoietic progenitor cells, and ccnd1(cyclin D1: G1/S-specific cyclin-D1) forms a complex with and functions as a regulatory subunit of CDK4 or CDK6, whose activity is required for cell cycle G1/S transition. Tumor markers were also upregulated at 5.75 months of age (Fig. 5G), but the effect of AFB1 on those tumor markers are stronger than HBx alone or HBx and AFB1 together. For comparison, we also provided the lipid metabolism markers and fibrosis genes at 5.75 months in Supplementary Fig. 2. Those results demonstrated a synergistic effect of AFB1 and HBx on the regulation of lipogenic factors and lipid metabolism related genes at 9 wpi/5 M and cell cycle/division-related genes at 12 wpi/5.75 M.

Co-localization of PCNA with caspase 3 in HBx zebrafish liver samples and human HBV positive HCC samples

We found the PCNA positive proliferative frequency and the TUNEL positive apoptotic cells were increasing with the progression of time, we could like to determine whether those two conditions happened in the same location or not. We performed the double fluorescence immunostaining using antibody against PCNA and active caspase 3. The results showed that PCNA was co-localized with a active caspase 3a in HBx or AFB1-treated HBx zebrafish liver (Fig. 6A) and human HBV positive HCC samples of stage I–II (Fig. 6B). This result indicated the proliferation and apoptotic events co-existed in both human HCC and zebrafish liver hyperplasia.

Discussion

Liver cancer or hepatocellular carcinoma (HCC) ranks as the third leading cause of mortality worldwide (Roberts and Gores, 2005; El-Serag and Rudolph, 2007). The morbidity and mortality in the surgical treatment of HCC patients in recent years has been reduced. However, the prognosis of HCC remains unsatisfactory; the 5-year survival rate of 25–49% after surgery is limited (Lu et al., 2011). Therefore, it is important to study carcinogenesis in animal models and develop drug screening platforms. Human hepatitis B virus (HBV) is one of the major etiological factors and risk factors for HCC (Bosch et al., 2004). The HBV X protein (HBx) is essential for virus replication *in vivo* and play a crucial role in the development of HCC (Cheng et al., 2007; Ng and Lee, 2011). In HBx transgenic mouse model, 80% incidence of HCC was observed at around 16-months of age (Wu et al., 2006). In transgenic fish, HCV transgenic fish treated with TAA developed HCC ten times faster than HCV transgenic mouse (Rekha et al., 2008). However, more than 99% of HBx transgenic fish develop only hepatic steatosis and liver degeneration within 8–10 months without any sign of HCC (Shieh et al., 2010). Aflatoxin B (AFB1) is one of the most prevalent carcinogens inducing liver cancer (Woo et al., 2011; Wogan et al., 2012). By treating the HBx transgenic fish with AFB1, we test the hypothesis of the synergistic effect between etiological factors, and examine the carcinogenesis by histological, immunostaining and molecular methods.

The zebrafish is an excellent model for delineating the mechanisms that underlie hepatocarcinogenesis and for use as a therapeutic drug-screening platform (Spitsbergen and Kent, 2003; Zon and Peterson, 2005; Lieschke and Currie, 2007). Many oncogenes have been shown to induce HCC in zebrafish, including *krasV12* (Nguyen et al., 2011, 2012), *xmrk* (Li et al., 2012), and human *RAF-1* (He et al., 2011), and the tumors induced in the zebrafish share many similar features with those occurring in humans (Li et al., 2012). Viral infections have been correlated to hepatocarcinogenesis. The expression of the HCV core protein combined with a treatment with the hepatotoxin thioacetamide (TAA) has been shown to induce HCC in zebrafish (Rekha et al., 2008). However, the overexpression of the HBx protein alone caused hepatic steatosis and liver degeneration but no signs of HCC in zebrafish (Shieh et al., 2010). Co-expression of HBx and HCV core antigen can induce the formation of intrahepatic cholangiocarcinoma in zebrafish providing evidence of the usefulness of studying synergistic effect between oncogenic factors using zebrafish model (Liu et al., 2012). In this study, we report the collaborative effect of HBx and AFB1 in causing steatosis, fibrosis and hyperplasia using a transgenic zebrafish model. To investigate proliferation or apoptosis were associated with enhanced cell proliferation or cell death, proliferation and death assays using proliferating cell nuclear antigen (PCNA) and active caspase 3 double fluorescence staining were

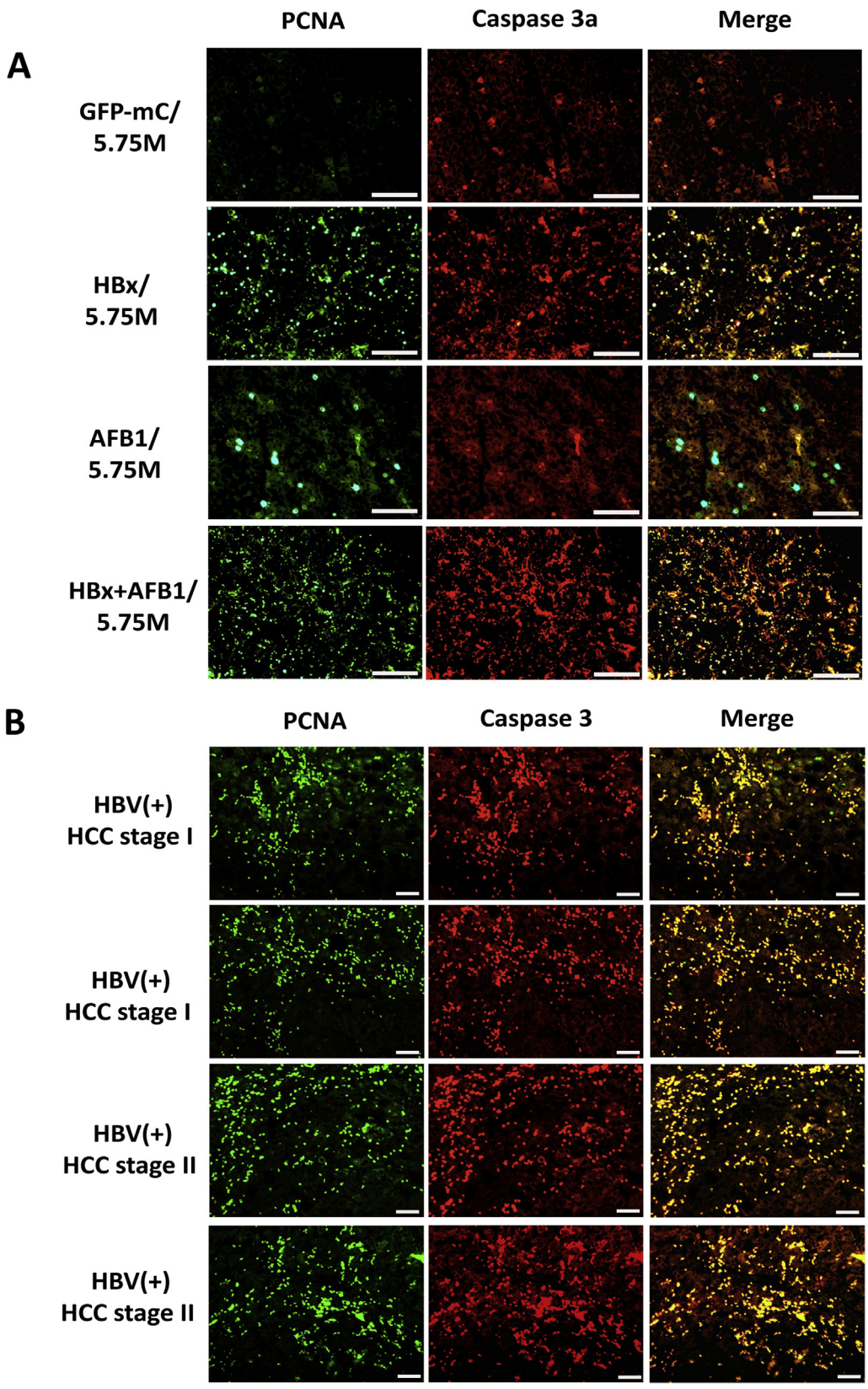

Fig. 6. Double immunofluorescence staining of PCNA and active caspase 3 in the liver sections of transgenic zebrafish and Human HCC sample (A) detection of proliferating and apoptotic cells in livers of 5.75-month-old EGFP-mCherry, HBx, AFB1, HBX + AFB1 fish (400×) and (B) human HCC livers of stage I–II (200×) by double immunofluorescence staining. The PCNA (green) positive cells are proliferating, and active caspase 3 (red) immuno-positive cells are considered apoptotic. Merge of both PCNA and active caspase 3a positive cells are shown as yellow. Scale bars = 50 μm. (For interpretation of the references to color in this figure legend, the reader is referred to the web version of the article.)

performed. PCNA was co-localized with caspase 3 in HBx or AFB1-treated HBx zebrafish liver and human HBV positive HCC samples of stage I–II, which indicated that they might be responsible for the process of liver cancer formation, which is similar in zebrafish and human.

There are many risk factors for developing HCC, and we tested two of them here for synergistic effects with HBx. Previously, AFB1 was used in rainbow trout to induce a high incidence of liver neoplasia (Bailey et al., 1996). Here, we demonstrated that AFB1 works synergistically with HBx to promote steatosis as early as 1 wpi/3 M, and finally developed into hyperplasia at 12 wpi/5.75 M in zebrafish. However, HBx and AFB1 alone can promote fibrosis, glycogen accumulation, and apoptosis and no synergistic effect between them was observed in those pathological situations. Using quantitative RT-PCR to analyze the expression of lipogenic factors, lipid metabolism related genes, fibrosis markers, tumor markers and cell cycle/division related genes, we discovered the synergistic effect between HBx and AFB1 on increasing the expression of most of the lipid metabolism related genes at 9 wpi/5 M and cell cycle/division related genes at 12 wpi/5.75 M. Our data provide evidence for the synergistic effects between different risk factors in hepatocarcinogenesis especially in promoting steatosis and hyperplasia.

In a mouse model, the HBx transgenic mice developed into tumor nodules with all the characteristics of hepatocellular adenomas at 22 weeks. Those nodules accumulated relatively high amounts of HBx protein and contained increased levels of glycogen (Zhu et al., 2004). PAS positivity had been correlated to longer survival rate and tumor volume doubling time in humans (Kitamura et al., 1993). In this study, both HBx transgenic fish treated with AFB1 and human patients with inflammation, cirrhosis, stages II–III of HCC and CC, exhibited significantly stronger glycogen accumulation than the normal liver by PAS staining. We suggest that PAS staining could be useful in assessing the prognosis of human patients. Our zebrafish model provides a robust platform for understanding the interplay between environmental signals and genetic factors in causing liver disease and combined with the clinical diagnosis. This animal model also provides new possibilities for screening potential therapeutics for fatty liver, hepatitis, cirrhosis, and liver cancer.

Acknowledgements

This research was supported by NRPGM (NSC 99-3112-B-400-010) and NSC grants (NSC 101-2321-B-400-017) provided to C.H.Y. Funding support from the National Health Research Institute provided to C.H.Y. is gratefully acknowledged. We would like to thank the Taiwan Zebrafish Core Facility at NTHU-NHRI site for providing the fish lines and resources, TZeTH is supported by grant 101-2321-B-400-014 from the National Science Council (NSC). The fellowship to Jeng-Wei Lu and the funding support to Dr. Chiou-Hwa Yuh from the Liver Disease Prevention & Treatment Research Foundation, Taiwan is highly acknowledged.

Appendix A. Supplementary data

Supplementary data associated with this article can be found, in the online version, at http://dx.doi.org/10.1016/j.acthis.2013.02.012.

References

Aguilar F, Harris CC, Sun T, Hollstein M, Cerutti P. Geographic variation of p53 mutational profile in nonmalignant human liver. Science 1994;264:1317–9.

Akriviadis EA, Llovet JM, Efremidis SC, Shouval D, Canelo R, Ringe B, et al. Hepatocellular carcinoma. Br J Surg 1998;85:1319–31.

Andre M, Ando S, Ballagny C, Durliat M, Poupard G, Briancon C, et al. Intestinal fatty acid binding protein gene expression reveals the cephalocaudal patterning during zebrafish gut morphogenesis. Int J Dev Biol 2000;44:249–52.

Bailey GS, Williams DE, Hendricks JD. Fish models for environmental carcinogenesis: the rainbow trout. Environ Health Perspect 1996;104(Suppl. 1):5–21.

Beasley RP, Hwang LY, Lin CC, Chien CS. Hepatocellular carcinoma and hepatitis B virus. A prospective study of 22 707 men in Taiwan. Lancet 1981;2:1129–33.

Bennett JW, Klich M. Mycotoxins Clin Microbiol Rev 2003;16:497–516.

Bosch FX, Ribes J, Diaz M, Cleries R. Primary liver cancer: worldwide incidence and trends. Gastroenterology 2004;127:S5–16.

Brechot C. Pathogenesis of hepatitis B virus-related hepatocellular carcinoma: old and new paradigms. Gastroenterology 2004;127:S56–61.

Chan TM, Chao CH, Wang HD, Yu YJ, Yuh CH. Functional analysis of the evolutionarily conserved cis-regulatory elements on the sox17 gene in zebrafish. Dev Biol 2009;326:456–70.

Cheng AS, Wong N, Tse AM, Chan KY, Chan KK, Sung JJ, et al. RNA interference targeting HBx suppresses tumor growth and enhances cisplatin chemosensitivity in human hepatocellular carcinoma. Cancer Lett 2007;253:43–52.

Denovan-Wright EM, Pierce M, Wright JM. Nucleotide sequence of cDNA clones coding for a brain-type fatty acid binding protein and its tissue-specific expression in adult zebrafish (*Danio rerio*). Biochim Biophys Acta 2000;1492:221–6.

El-Serag HB, Mason AC, Key C. Trends in survival of patients with hepatocellular carcinoma between 1977 and 1996 in the United States. Hepatology 2001;33:62–5.

El-Serag HB, Rudolph KL. Hepatocellular carcinoma: epidemiology and molecular carcinogenesis. Gastroenterology 2007;132:2557–76.

He S, Krens SG, Zhan H, Gong Z, Hogendoorn PC, Spaink HP, et al. A DeltaRaf1-ER-inducible oncogenic zebrafish liver cell model identifies hepatocellular carcinoma signatures. J Pathol 2011;225:19–28.

Her GM, Chiang CC, Chen WY, Wu JL. In vivo studies of liver-type fatty acid binding protein (L-FABP) gene expression in liver of transgenic zebrafish (*Danio rerio*). FEBS Lett 2003;538:125–33.

Hiruma S, Gopalan-Kriczky P, Qin G, Gaughan JP, Lotlikar PD. Differential effects of acetaminophen pretreatment on hepatic aflatoxin B(1)-DNA binding, cellular proliferation, and aflatoxin B1-induced hepatic foci in rats and hamsters. Cancer Lett 2001;170:117–24.

Hsu IC, Metcalf RA, Sun T, Welsh JA, Wang NJ, Harris CC. Mutational hotspot in the p53 gene in human hepatocellular carcinomas. Nature 1991;350:427–8.

Jeannot E, Boorman GA, Kosyk O, Bradford BU, Shymoniak S, Tumurbaatar B, et al. Increased incidence of aflatoxin B1-induced liver tumors in hepatitis virus C transgenic mice. Int J Cancer 2011;130:1347–56.

Kew MC. Synergistic interaction between aflatoxin B1 and hepatitis B virus in hepatocarcinogenesis. Liver Int 2003;23:405–9.

Kew MC. Hepatitis B virus x protein in the pathogenesis of hepatitis B virus-induced hepatocellular carcinoma. J Gastroenterol Hepatol 2011;26(Suppl. 1):144–52.

Kitamura S, Tatsuta M, Yamamoto R, Iishi H, Kaji I, Kasugai H, et al. Prognostic value of periodic Acid-schiff (pas) staining of fine-needle aspirates from patients with primary hepatocellular-carcinoma. J Gastroenterol Hepatol 1993;3:245–51.

Kwan KM, Fujimoto E, Grabher C, Mangum BD, Hardy ME, Campbell DS, et al. The Tol2kit: a multisite gateway-based construction

kit for Tol2 transposon transgenesis constructs. Dev Dyn 2007;236:3088–99.
Li CH, Wang YJ, Dong W, Xiang S, Liang HF, Wang HY, et al. Hepatic oval cell lines generate hepatocellular carcinoma following transfection with HBx gene and treatment with aflatoxin B1 in vivo. Cancer Lett 2011;311:1–10.
Li Z, Huang X, Zhan H, Zeng Z, Li C, Spitsbergen JM, et al. Inducible and repressable oncogene-addicted hepatocellular carcinoma in Tet-on xmrk transgenic zebrafish. J Hepatol 2012;56:419–25.
Lian M, Liu Y, Yu SZ, Qian GS, Wan SG, Dixon KR. Hepatitis B virus x gene and cyanobacterial toxins promote aflatoxin B1-induced hepatotumorigenesis in mice. World J Gastroenterol 2006;12:3065–72.
Lieschke GJ, Currie PD. Animal models of human disease: zebrafish swim into view. Nat Rev Genet 2007;8:353–67.
Liu W, Chen JR, Hsu CH, Li YH, Chen YM, Lin CY, et al. A zebrafish model of intrahepatic cholangiocarcinoma by dual expression of hepatitis B virus X and hepatitis C virus core protein in liver. Hepatology 2012;56:2268–76.
Lu JW, Chang JG, Yeh KT, Chen RM, Tsai JJ, Hu RM. Overexpression of Thy1/CD90 in human hepatocellular carcinoma is associated with HBV infection and poor prognosis. Acta Histochem 2011;113:833–8.
Lu JW, Hsia Y, Yang WY, Lin YI, Li CC, Tsai TF, et al. Identification of the common regulators for hepatocellular carcinoma induced by hepatitis B virus X antigen in a mouse model. Carcinogenesis 2012;33:209–19.
Luyendyk JP, Copple BL, Barton CC, Ganey PE, Roth RA. Augmentation of aflatoxin B1 hepatotoxicity by endotoxin: involvement of endothelium and the coagulation system. Toxicol Sci 2003;72:171–81.
Marrero CR, Marrero JA. Viral hepatitis and hepatocellular carcinoma. Arch Med Res 2007;38:612–20.
McGlynn KA, London WT. Epidemiology and natural history of hepatocellular carcinoma. Best Pract Res Clin Gastroenterol 2005;19:3–23.
Morgan TR, Mandayam S, Jamal MM. Alcohol and hepatocellular carcinoma. Gastroenterology 2004;127:S87–96.
Ng SA, Lee C. Hepatitis B virus X gene and hepatocarcinogenesis. J Gastroenterol 2011;46:974–90.
Nguyen AT, Emelyanov A, Koh CH, Spitsbergen JM, Lam SH, Mathavan S, et al. A high level of liver-specific expression of oncogenic Kras(V12) drives robust liver tumorigenesis in transgenic zebrafish. Dis Model Mech 2011;4:801–13.
Nguyen AT, Emelyanov A, Koh CH, Spitsbergen JM, Parinov S, Gong Z. An inducible kras(V12) transgenic zebrafish model for liver tumorigenesis and chemical drug screening. Dis Model Mech 2012;5:63–72.
Pang R, Tse E, Poon RT. Molecular pathways in hepatocellular carcinoma. Cancer Lett 2006;240:157–69.
Peng Z, Zhang Y, Gu W, Wang Z, Li D, Zhang F, et al. Integration of the hepatitis B virus X fragment in hepatocellular carcinoma and its effects on the expression of multiple molecules: a key to the cell cycle and apoptosis. Int J Oncol 2005;26:467–73.
Rekha RD, Amali AA, Her GM, Yeh YH, Gong HY, Hu SY, et al. Thioacetamide accelerates steatohepatitis, cirrhosis and HCC by expressing HCV core protein in transgenic zebrafish *Danio rerio*. Toxicology 2008;243:11–22.
Roberts LR. Sorafenib in liver cancer – just the beginning. N Engl J Med 2008;359:420–2.
Roberts LR, Gores GJ. Hepatocellular carcinoma: molecular pathways and new therapeutic targets. Semin Liver Dis 2005;25:212–25.
Robinson WS. The role of hepatitis B virus in the development of primary hepatocellular carcinoma: part I. J Gastroenterol Hepatol 1992;7:622–38.
Seeff LB, Hoofnagle JH. Epidemiology of hepatocellular carcinoma in areas of low hepatitis B and hepatitis C endemicity. Oncogene 2006;25:3771–7.
Shieh YS, Chang YS, Hong JR, Chen LJ, Jou LK, Hsu CC, et al. Increase of hepatic fat accumulation by liver specific expression of Hepatitis B virus X protein in zebrafish. Biochim Biophys Acta 2010;1801:721–30.
Siegel AB, Olsen SK, Magun A, Brown Jr RS. Sorafenib: where do we go from here? Hepatology 2010;52:360–9.
Spitsbergen JM, Kent ML. The state of the art of the zebrafish model for toxicology and toxicologic pathology research – advantages and current limitations. Toxicol Pathol 2003;31(Suppl.): 62–87.
Tarantino G, Saldalamacchia G, Conca P, Arena A. Non-alcoholic fatty liver disease: further expression of the metabolic syndrome. J Gastroenterol Hepatol 2007;22:293–303.
Tseng WF, Jang TH, Huang CB, Yuh CH. An evolutionarily conserved kernel of gata5, gata6, otx2 and prdm1a operates in the formation of endoderm in zebrafish. Dev Biol 2011;357:541–57.
Wild CP, Jansen LA, Cova L, Montesano R. Molecular dosimetry of aflatoxin exposure: contribution to understanding the multifactorial etiopathogenesis of primary hepatocellular carcinoma with particular reference to hepatitis B virus. Environ Health Perspect 1993;99:115–22.
Wild CP, Turner PC. The toxicology of aflatoxins as a basis for public health decisions. Mutagenesis 2002;17:471–81.
Wogan GN, Kensler TW, Groopman JD. Present and future directions of translational research on aflatoxin and hepatocellular carcinoma. A review. Food Addit Contam Part A 2012;29:249–57.
Woo LL, Egner PA, Belanger CL, Wattanawaraporn R, Trudel LJ, Croy RG, et al. Aflatoxin B1-DNA adduct formation and mutagenicity in livers of neonatal male and female B6C3F1 mice. Toxicol Sci 2011;122:38–44.
Wu BK, Li CC, Chen HJ, Chang JL, Jeng KS, Chou CK, et al. Blocking of G1/S transition and cell death in the regenerating liver of Hepatitis B virus X protein transgenic mice. Biochem Biophys Res Commun 2006;340:916–28.
Zhu H, Wang Y, Chen J, Cheng G, Xue J. Transgenic mice expressing hepatitis B virus X protein are more susceptible to carcinogen induced hepatocarcinogenesis. Exp Mol Pathol 2004;76: 44–50.
Zhu S, Lee JS, Guo F, Shin J, Perez-Atayde AR, Kutok JL, et al. Activated ALK collaborates with MYCN in neuroblastoma pathogenesis. Cancer Cell 2012;21:362–73.
Zon LI, Peterson RT. In vivo drug discovery in the zebrafish. Nat Rev Drug Discov 2005;4:35–44.